Tripathi, Tripurari Sharan; Karppinen, Maarit

Mixed-Anion Compounds

Published in:
Advanced Materials Interfaces

DOI:
10.1002/admi.202100146

Published: 09/06/2021

Document Version
Publisher's PDF, also known as Version of record

Please cite the original version:
Tripathi, T. S., & Karppinen, M. (2021). Mixed-Anion Compounds: An Unexplored Playground for ALD Fabrication. *Advanced Materials Interfaces*, *8*(11), Article 2100146. https://doi.org/10.1002/admi.202100146

ADVANCED MATERIALS INTERFACES
www.advmatinterfaces.de

Mixed-Anion Compounds: An Unexplored Playground for ALD Fabrication

Tripurari Sharan Tripathi and Maarit Karppinen**

For decades the most successful approach towards new inorganic material innovations for next-generation devices has been to manipulate the cation composition. As this cation-centric material development is inevitably approaching its saturation, new chemistries are needed to maintain the pace of technological progress. One of the new chemistry approaches is to play with the anions instead of the cations. Moreover, advances in fabrication techniques are needed to address the endeavors to shrink the device and component dimensions. Here, the combination of mixed-anion chemistries, such as oxychalcogenides or carbopnictides, and the state-of-the-art atomic layer deposition (ALD) thin-film technology are highlighted. The unique bottom-up material building mode of ALD can lead to scientifically exciting but at the same time industry-feasible material innovations. In this brief review, the present status and prospects, and the challenges of this emerging field are discussed.

1. Introduction

The progress in many advanced technologies relies on the development of new active materials with demanded functionalities. New materials with unorthodox properties are needed both to improve the existing and to enable the next-generation technologies. This strong positive challenge continuously urges materials scientists to search for entirely new material families. Moreover, advances in fabrication techniques are needed to address the continuously shrinking device and component dimensions. Conventionally the new-material search has centered around single-anion (homo-anionic) compounds, such as pure metal oxides, chalcogenides (sulfides, selenides, tellurides), or pnictides (nitrides, phosphides, arsenides), where the properties are fine-tuned by controlling the cation (metal) composition for doping, etc.

As this cation-centric new material research is approaching its saturation, researchers have started to look for novel material chemistries, such as the so-called mixed-anion (multi-anion or hetero-anionic) compounds.[1–6] In this strongly emerging material family, the play with the size, charge, electron configuration, electronegativity, and polarizability of different anionic species is believed to provide us with an exciting way to control the local distortions and band structures, and thereby to create unique structural, chemical, electronic, optical, and magnetic states. In the best case, this would lead us to phenomena inaccessible through other compositional tuning approaches. Both the cation and anion manipulation may be used to control the charge balance through aliovalent substitutions, but by combining multiple anions around a single cation site we can in a more straightforward manner create diversity within the cation coordination sphere. To mention few examples, anion mixing in the coordination sphere could be used to introduce a spread of binding energies to control the anionic conductivity, or to create cis/trans isomerization effects.[1] For local symmetry breaking, we could look for anisotropic anions, such as O_2^{2-} or S_2^{2-}. As for the bandgap tuning via anion mixing, one of the early examples is the Ta_2O_5-TaON system for photocatalysis application.[7] More recently, the oxychloride compound Bi_4NbO_8Cl was highlighted as a new stable visible light responsive photocatalyst for water splitting.[8]

The anion components for the multi-anion compounds could be from the different groups of the Periodic Table, for example, oxyhalogenides or carbopnictides, or from the same group, for example, oxysulfides, or even a combination of inorganic and organic anions. As of now, the mixed-anion compounds are yet far out-numbered by the single-anion compounds, and there is plenty of room to explore these materials, in particular, provided that we could fabricate the materials in high-quality thin-film form, most demanded for their future application. Prominent examples of the specific applications of the mixed-anion materials include (**Figure 1**): LiPON for microbattery,[9,10] (Ga,Zn)(N,O) for water splitting or photovoltaics,[11] and BiCuSeO[12,13] and Pb(Se,Te)[14] for thermoelectrics. Mixed-anion compounds such as $Na_3BH_4B_{12}H_{12}$ have also shown superionic conduction owing to the highly disordered cations and continuous migration paths in the structure; this specific $Na_3BH_4B_{12}H_{12}$ compound with a room-temperature conductivity of 0.5×10^{-3} S cm^{-1} could provide us a light-weight solution for the electrolyte in Na-based all solid-state batteries.[15] In **Figure 2**a, the total numbers of publications on some of the most important mixed-anion compounds are shown.

One of the obstacles of the research in this field is the relatively demanding synthesis of multi-anion compounds. The major difficulty in their direct synthesis is in the different

Dr. T. S. Tripathi, Prof. M. Karppinen
Department of Chemistry and Materials Science
Aalto University
Espoo FI-00076, Finland
E-mail: tripurari.tripathi@aalto.fi; maarit.karppinen@aalto.fi

The ORCID identification number(s) for the author(s) of this article can be found under https://doi.org/10.1002/admi.202100146.

DOI: 10.1002/admi.202100146

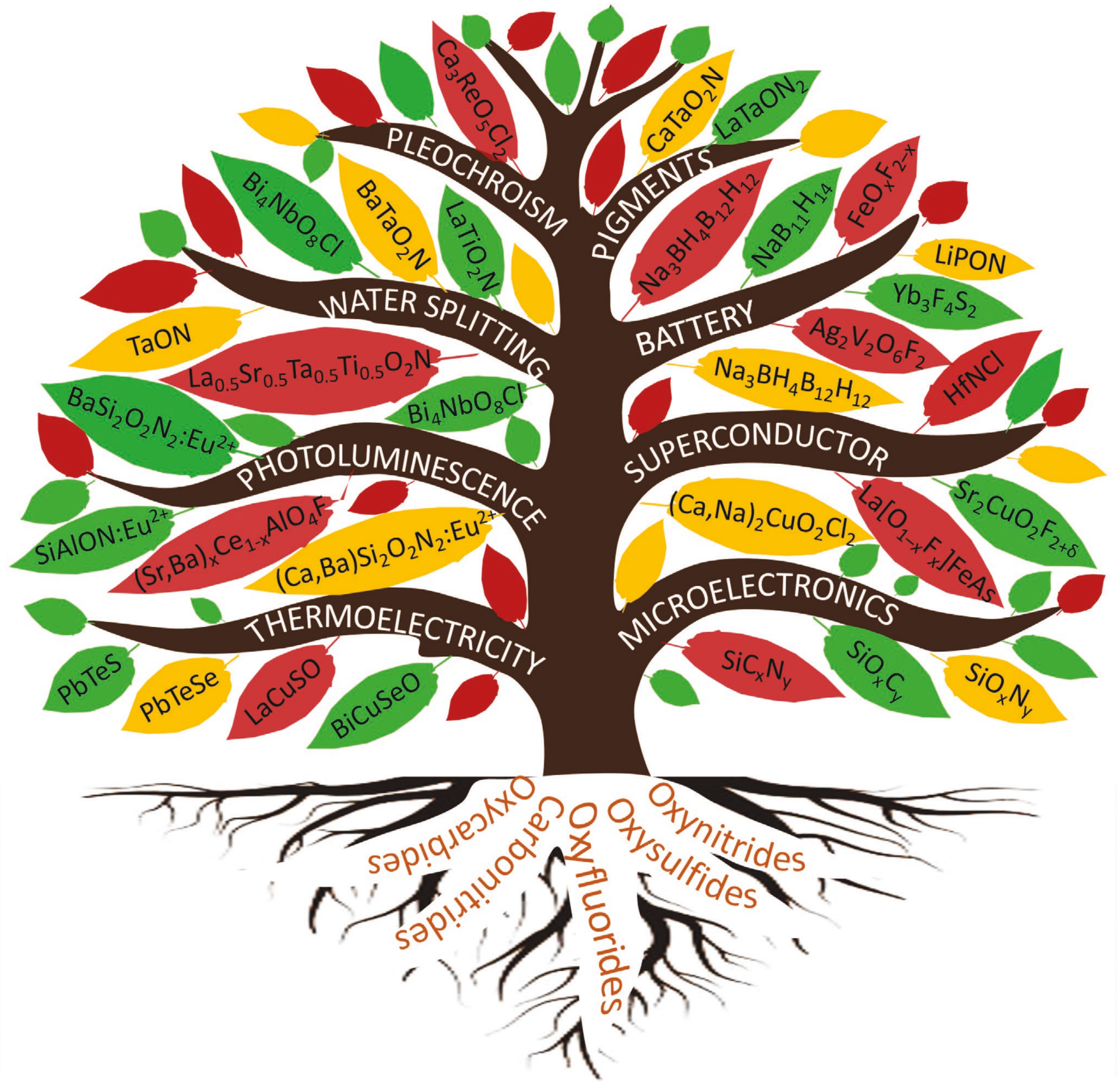

Figure 1. Examples of possible application areas of mixed-anion materials.

volatilities (and hence optimal synthesis conditions) of the precursors for the common non-metals forming the anions, for example, hydrogen, carbon, nitrogen, pnictides, oxygen, chalcogenides, and halogens. Hence, controlled atmosphere synthesis conditions, for example, vacuum or gas flows (O_2, F_2, NH_3, H_2S, etc.), are preferred. Accordingly, gas-phase thin-film techniques are highly relevant choices for the mixed-anion compound fabrication, in particular as many of their advanced applications would require high-quality thin films.

Atomic layer deposition (ALD) is state-of-the-art thin-film technology for many industrially important binary metal oxides, sulfides, and nitrides.[16–18] Along with its increasing impact especially in microprocessors and digital memory devices, ALD is currently the fastest-growing thin-film deposition technique in general. In ALD, the atomic-level film thickness and composition control, as well as the large-area homogeneity and superior conformality over complex surface structures, stem from the self-limited gas-surface reactions of sequentially pulsed gaseous precursors. Owing to the digital control over the precursor supply, the ALD technique is rather fundamentally well suited for the anion mixing, thereby permitting the fine-tuning of the mixed-anion thin films. In Figure 2b, we summarize the number of annually published ALD papers on mixed-anion compounds; the first paper is for GaAs/GaP thin films by Ozeki published in 1990.[19] Despite the steadily increasing interest in these materials, there are no reviews on

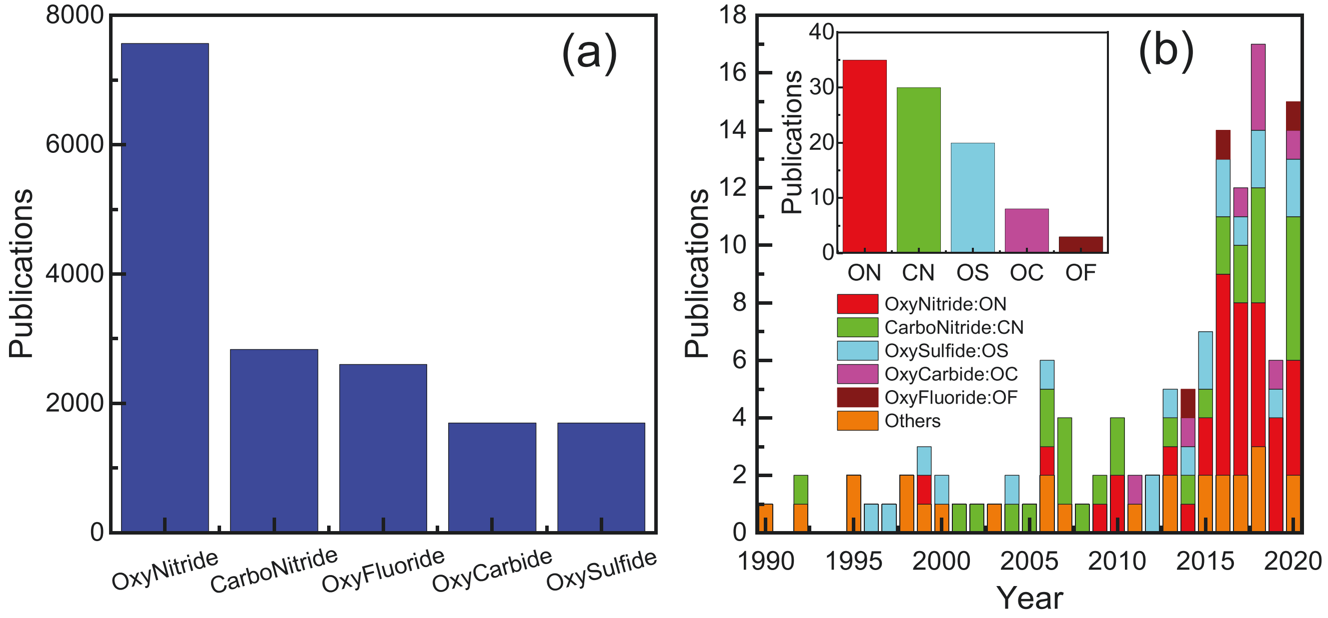

Figure 2. a) All publications: total number of papers published on the five most important mixed-anion chemistries (Web of Science search 22.12.2020); b) ALD publications: annually published papers on ALD-fabricated mixed-anion thin films; inset shows the division of the ALD papers between the most important mixed-anion chemistries.

their fabrication through ALD or any other traditional thin-film deposition technique. Therefore, this review aims to present the current state-of-the-art in the field, and in particular to summarize i) the available ALD processes developed for mixed-anion compounds, and ii) the anion precursors utilized in these processes, iii) highlight some promising functionalities of the ALD-fabricated mixed-anion thin films, and iv) discuss the advantages and limitations of ALD in the application space of these materials. In the following, we will first devote a short chapter to the basics of the ALD technique (Chapter 2), and then discuss the fabrication strategies and precursor choices for the reported mixed-anion ALD processes (Chapter 3). Then, towards the end, we discuss examples of state-of-the-art ALD-grown mixed-anion thin films in Chapter 4, and finally, in Chapter 5 provide a summary and outlook for the future perspectives and challenges in this scientifically exciting and industrially important field.

2. Atomic Layer Deposition in Brief

ALD thin-film technology is one of the cornerstones of modern microelectronics and beyond. It yields high-quality conformal inorganic thin films (e.g., Al_2O_3 or HfO_2) with excellent precision for thickness and uniformity. The technique relies on self-limiting gas-surface reactions of vaporized precursors (e.g., $Al(CH_3)_3$ and H_2O for Al_2O_3) sequentially introduced in a vacuum reactor; carrier gas (e.g., N_2) is used to aid the precursor transportation and separation of the different precursor exposures. In its simplest case, an ALD cycle is composed of the following sequence of exposures: 1) first (metal-bearing) precursor, 2) inert gas purge, 3) second precursor or so-called co-reactant, and 4) inert gas purge, see **Figure 3**. This basic ALD cycle is repeated as many times as needed to grow the thin film with the desired thickness. In an ideal case, each cycle produces a monolayer of the targeted material. In practice, however, the growth-per-cycle (GPC) is often less due to,

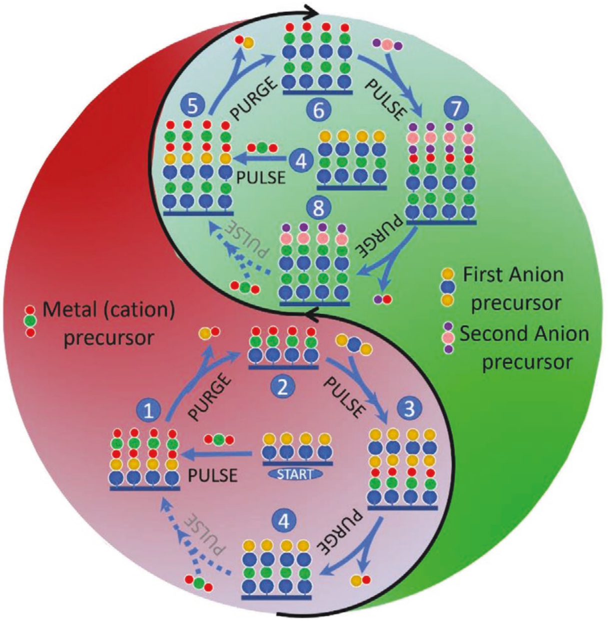

Figure 3. (Left, purple) Schematic illustration of the basic ALD cycle consisting of four steps; Step 1: introduction of the first (metal-bearing) precursor that chemisorbs to reactive surface sites until full surface coverage; Step 2: purge of the side product(s) and excess precursor molecules with an inert gas pulse (e.g., N_2); Step 3: introduction of the second precursor (typically the oxygen, nitrogen or sulfur source, e.g. O_3, H_2O, NH_3, or H_2S); Step 4: purge with an inert gas pulse. These four steps are repeated to achieve the desired film thickness. (Right, green) Schematic illustration of the addition of the second anion precursor to the basic ALD process; the combination of these cycles creates the so-called supercycle.

for example, steric hindrance of the large ligands in the precursor molecules.

Typically, GPC values of the order of 1 Å cycle^{-1} are achieved.[20] Initially, ALD was used in the niche applications where the quality of the films was the prime criterion. However, as the gadgets are continuously becoming smaller and the integration density of components is increasing, such that the slow growth rate is no longer a constraint and thus ALD has already been widely commercialized.[21] In general, it is superiorly suited to address most if not all of the fabrication challenges faced in frontier electronics, optics, and photovoltaic applications.[22–25] For several proprietary applications, the required conformal coatings on ultrahigh-aspect-ratio structures without gradients in thickness or composition have already been achieved by ALD.[26,27]

The majority of ALD materials that have been deposited are metal oxides because of the commercial demand for thin-film dielectrics.[21] However, novel applications in areas such as energy storage,[23] catalysis,[28] and nanophotonics[29] are emerging. For example, ALD is considered a highly suitable manufacturing technique for the buffer layers in solar cells because the method allows for the uniform deposition of large-area thin films, which makes it easier to control the composition of the thin films.[30,31] Furthermore, ALD in combination with its purely organic variant viz. molecular layer deposition (MLD)[29] is also gaining momentum for promising applications. The aforementioned widely documented capabilities of the ALD technique would be of fundamental importance in the emerging field of mixed-anion compounds as well, considering, for example, the important aspects related to stoichiometry control, defect chemistry, and morphological properties.

The possibility to grow thin films of well-defined composition, density, thickness, uniformity, and conformality on 3D topologies is due to a most characteristic and unique feature of ALD, that is, the self-limiting growth mode.[32] Conformality of the films on ultrahigh-aspect-ratio structures is often a critical factor in choosing ALD over competing for deposition techniques such as CVD, PVD, and sputtering for the fabrication of conformal coatings. The sufficiently large precursor pulse duration allows the dispersion of precursor into deep trenches to complete the gas-surface reaction over the entire surface. The self-limiting growth characteristics restrict the reactions to only one layer of the precursor resulting in the highly conformal coatings on high aspect ratio and 3D structured substrate morphologies.

Precise composition control is another important benefit of the self-saturating growth mode of ALD which allows the unique "one-layer at a time" growth. For both the compounds containing more than two elements/components, the composition tuning is in principle achieved by designing so-called supercycles, which are composed of multiple binary ALD processes (Figure 3).[33–36] This approach is commonly applied not only for the mixed-anion compounds, but for the mixed-cation compounds, including the cation-doped compounds. However, it should be noted that experimentally it is sometimes difficult to achieve/verify the perfect mixing of the components and distinguish the mixed-cation or mixed-anion compounds from corresponding nanoscale multilayer structures or so-called nanolaminates. Finally, the alternate precursor exposure allows the use of highly reactive precursors (as the unwanted gas-phase reactions are avoided), which reduces the thermal budget. Usually, in ALD fabrications a wide temperature range is realized where the GPC value remains approximately fixed for the films. This facilitates the successful fabrication of multilayer structures.

Table 1. ALD precursors used for anions.

Group	Element	Precursors
Carbon	C	CCl_3[37] CF_3,[38] CBr_3,[39] C_2H_4,[40]
Oxide	O	O_2, O_3, H_2O, H_2O_2*, CH_3OH, C_2H_5OH, NO_2[32]
Chalcogen	S	S,[41,42] H_2S[43–46] 1-propanethiol,[47] di-*tert*-butyl disulfide,[48]
	Se	Se,[49] H_2Se,[50–53] $(Et_3Si)_2Se$,[54–56] $(Me_3Si)_2Se$[57–60]
	Te	Te,[61] H_2Te,[62] $Te(t\text{-}Bu)_2$[59,63] $(Et_3Si)_2Te$[55] $Te_2(n\text{-}C_4H_9)_2$[64] methylallyltelluride (MATe),[65] $(Me_3Si)_2Te$[58,66,67]
Pnictogen	N	NH_3, H_2/NH_3[68,69] N_2, H_2/N_2[26,70] N_2H_4[71,72] $(CH_3)NH_2$, $^tBuNH_2$, CH_2CHCH_2NH,[73] diethyl phosphoramidate $H_2NP(O)(OC_2H_5)_2$ (DEPA)[74]
	P	PH_3[75–77]
	As	AsH_3[78,79]
	Sb	$SbCl_3$, $(CH_3)_2N)_3Sb$[80]
	Bi	$BiCl_3$[80]
Halogen	F	HF, TiF_4[81–84]
	Cl	HCl
	Br	HBr[85]
	I	I_2, SnI_4[86]

3. Fabrication Process Strategies and Precursors

The variety of the precursors used as sources of the anions is extensive; these are summarized in **Table 1**. Considering the mixing of the multiple anions, most of the ALD fabrication processes fall into the following four categories (shortly described below): i) supercycle approach, ii) exchange reaction method, iii) plasma-enhanced ALD (PE-ALD), and iv) spatial ALD (SALD). In **Table 2**, we list the ALD processes so far reported for the fabrication of mixed-anion compounds. We also like to mention—for a reference—the comprehensive database for ALD processes published in the atomiclimits site (https://www.atomiclimits.com/alddatabase/).

3.1. Supercycle Approach

The most common ALD approach for ternary compounds including the present mixed-anion compounds is to mix two (or more) basic ALD cycles in an appropriate ratio into a single supercycle, as was illustrated in Figure 3. For example, for the fabrication of Zn(O, S) films by ALD, Jeon et al.[87] used three different mixing conditions of ZnO:ZnS, that is, (4:1), (5:5), and (1:4), to control the mixing ratio of oxygen and sulfur in their Zn(O,S) films. They used diethylzinc (DEZ) as the source for zinc and H_2O and H_2S as the sources for oxygen and sulfur. Similarly, in another approach, AlO_xF_y films were deposited by

Table 2. ALD processes reported for mixed-anion compounds.

Compound	Cation precursor	Anion precursor	ALD window (W)/Dep. T (DT) [°C]	GPC [Å]	Ref.
MoC_xN_y	$Mo(N^tBu)_2(NMe_2)_2$	N_2/H_2 plasma	80–300 (DT)	0.36–0.6	[99]
SiC_xN_y	Si_2Cl_6	CH_3NH_2 plasma	400 (DT)	1.0	[100]
	$(Me)_3(Vi)_3(NSiH_2)_3$	N_2 plasma	200 (DT)	–	[101,102]
	$(^iPr)_3(NSiH_2)_3$	NH_3 plasma	200 (DT)	–	[103]
TaC_xN_y	$Ta(NEt_2)_3(N^tBu)$	CH_4/H_2 plasma	200 (DT)	0.4–0.5	[104]
		H_2 plasma	100–400 (DT)	0.5–1.0	[105]
		NH_3 plasma	100–400 (DT)	0.5–4.0	[106]
		H_2 plasma	200–260 (W)	0.35	[107]
	$Ta(N^tAm)[(NMe_2)]_3$	H_2, Ar/H_2 plasma	350 (DT)	0.9–1.0	[108]
$TaAlC_xN_y$	$TaCl_5$ or $TaBr_5$	NH_3, $AlMe_3$	250–400 (DT)	0.8–0.9	[109]
TiC_xN_y	$Ti(NMe_2)_4$	H_2, NH_3, H_2/CH_4 plasma	100–300 (DT)	1.0–1.3	[110]
	$TiCl_4$	$AlH_2(N^tBuCH_2CH_2NC_4H_8)$	220–400 (DT)	1.6–2.0	[111]
WC_xN_y	$W(CpEt)(CO)_2(NO)$	H_2 plasma	100–400 (DT)	0.17–0.28	[112]
	$W(MeCp)(CO)_2(NO)$	NH_3 plasma	250–450 (DT) 300–350 (W)	0.49–0.56	[113]
	$W(N^tBu)_2(NMe_2)_2$	H_2 plasma	300 (DT)	1.2	[114]
	WF_6	NH_3; triethylboron (Et_3B)	300–400 (DT) 300–350 (W)	0.8–0.9	[115–121]
		CH_4; NH_3; H_2	250 (DT)	–	[122]
ZrC_xN_y	TDMAZr	5% H_2, 95% N_2	150 (DT)	–	[123,124]
SiO_xC_y	$(Cl_3Si)CH_3$	H_2O	Room temperature	0.5	[125,126]
	DMADMSE	O_3	110	0.2	[127–129]
	OMCTS	O_2; Ar; H_2 plasmas	100–400	0.3–1.05	[130]
	TMS	O_2 plasma	–	–	[131]
	Si_2Cl_6	CO or CO/O_2 plasma	400	–	[100]
SiO_xN_y	BDEAS	NH_3 plasma	300	–	[132]
SnO_xN_y	$Sn(NMe_2)_4$	H_2O, N_2 plasma	200 (DT)	0.55–0.8	[133]
ZrO_xN_y	TDMAZr	N_2/H_2 plasma, NH_3 plasma	150, 250 (DT)	0.51	[124,134,135]
NbN_xO_y	TBTDEN	H_2 plasma	35 0(DT)	0.46	[136]
AlO_xN_y	$Al_2(NMe_2)_6$	NH_3, H_2O	200 (DT)	0.8	[137,138]
	$AlMe_3$	NH_3+ O_2 plasma	185, 400–450 (DT)	0.87–1.0	[139,140]
HfO_xN_y	$Hf(Hf(N((Et)Me)_4))$	NH_3, H_2O	200 (DT)	–	[141–143]
GaO_xN_y	TMG	O_2, NH_3 plasma	200 (DT)	0.4–0.7	[144,145]
TiO_xN_y	$Ti(NMe_2)_4$,	N_2 plasma, NH_3	100–300 (DT)	0.7	[146–150]
	$Ti(OiPr)_4$	NH_3 plasma	190–270 (W)	0.3–0.35	
	$TiCl_4$	NH_3, NH_4OH; O_2	250–450 (DT)	0.2–0.3	[151–155]
LiPON	LTB	Me_3P +H_2O, N_2, plasma N_2	250 (DT)	1.05	[156–158]
		$P(NMe_2)_3$, O_2+NH_3	350–500 (DT)	0.5–2.1	[159]
	$LiN(SiMe_3)_2$	$PO(NH_2)(OEt)_2$	270–310 (W)	0.7	[74]
Li_2PO_2N	LTB		250–300	0.15–0.9	[160]
NaPON	STB		250–400	0.2–0.5	[161]
MoON	$MoO_2(^tBuAMD)_2$	O_3	120–270 (DT)	0.2–0.3	[162]
MoO_xN_y	$Mo(CO)_6$	O_3; NH_3	170 (DT)		[163]
MnO_xN_y	$Mn(CpEt)_2$; $Mn(EtCp)_2$	NH_3 plasma	225–300 (W)	0.39	[164]
TaO_xN_y	$Ta(NEtMe)_2(N^iPr)$, $Ta(N^iPr)(NEtMe)_2$	Ar+$N_2/NH_3/H_2$ gas mixture	400 (DT)	–	[165]
	$TaCl_5$	H_2O; NH_3	-	–	[166]

Table 2. Continued.

Compound	Cation precursor	Anion precursor	ALD window (W)/Dep. T (DT) [°C]	GPC [Å]	Ref.
	$Ta(N(Me)_2)_5$	CH_3NHNH_2; H_2O; N_2	175–280 (W)	0.87–1.04	[167,168]
ZnO_xN_y	$ZnEt_2$	H_2O; NH_3	150 (DT)	–	[169]
ZnO_xB_y		H_2O; $B(O^iPr)_3$	150 (DT)	–	[170]
		H_2O; B_2H_6	105–165 (W)	2.8	[171]
ZnO_xP_y		H_2O, $PO(OMe)_3$	160–220	1.6–1.8	[172]
		O_3, $P(OMe)_3$	250 (DT)	1.7	[173]
AlO_xP_y	$AlCl_3$; $Al(O^nPr)_3$	H_2O, O_3; $(CH_3)_3COH$; P_2O_5	150–500 (DT)	0.15–1.3	[65,174–181]
CaO_xP_y	$Ca(thd)_2$	$(CH_3O)_3PO$; O_3; H_2O	250–400(DT)	0.3–0.6	[182]
MgO_xP_y	$Mg(EtCp)_2$	TDMAP; H_2O & O_2 plasma	125–300 (DT)	1.3	[183]
SnO_xP_y	$Sn(NMe_2)_4$	H_2O, $PO(OMe)_3$; O_3	200–250 (DT)	1.23–1.84	[184]
$GaAs_xP_y$	$GaMe_3$	AsH_3, PH_3	460–550 (DT)	0.5–1.0	[19]
LiO_xF_y	LTB	HFAA, TiF_4	220 (DT)	–	[185]
AlO_xF_y	$AlMe_3$	H_2O, HF	150 (DT)	–	[88]
ZnO_xF_y	$ZnEt_2$	H_2O, HF+H_2O	140 (DT)	2.1–2.5	[186]
BiOCl	$BiCl_3$	O_3	130, 300 (DT)	0.1–0.2	[187]
$ZnAl_xO_yS_z$	$ZnCl_2$; $AlCl_3$	H_2O, H_2S	500(DT)	0.39;0.79	[188]
ZnO_xS_y	$ZnEt_2$	O_2/Ar plasma, H_2S	120–220 (W)	1.2–2.5	[189]
		H_2O, H_2S	100–225 (DT)	1.0–2.0	[31,87,96,190–197]
	$ZnEt_2$; $ZnMe_2$	H_2O+O_2, H_2S	100–300 (DT)	1.05	[198,199]
Y_2O_2S	$Y(thd)_3$	H_2S	350–425 (DT)		[200]
$YO_xS_yEu_z$	$Y(MeCp)_3$; $Eu(thd)_3$	H_2S, O_3+H_2O	300 (DT)		[201]
CdO_xS_y	$CdCl_2$	H_2S, H_2O	140 (DT)	1.0	[202]
InO_xS_y	$In(acac)_3$	H_2S, Ar/O_2 plasma	160 (DT)	0.4–1.4	[89,90,203]
SnO_xS_y	$Sn(dmamp)_2$	H_2S, H_2O	100–180 (DT)	0.42–0.56	[204]
MoOSe	$Mo(CO)_6$	$(Me_3Si)_2Se$	167 (DT)	2.0	[57]
ZnS_xSe_y	Zn	H_2S, H_2Se	400 (DT)	2.7	[205]
	$ZnCl_2$	H_2S, Se	400 (DT)		[206]
	$ZnMe_2$	H_2S, H_2Se	150–225 (W)	2.71	[207,208]
SrS_xSe_y	$Sr(thd)_2$	H_2S, Se	380 (D)		[206]
$GeSb_xSe_yTe_z$	$Ge(OEt)_4$; $Sb(OEt)_3$	$Se(SiMe_3)_2$;$Te(SiMe_3)_2$	70 (DT)		[58,209]
$CdSe_xTe_y$	Cd	Se, Te	150–350		[210]
$SbSe_xTe_y$	$Sb(NMe_2)_3$	$Se(SiMe_3)_2$, Te^tBu_2	80–300	9.98	[59]
$PbSe_xTe_y$	$Pb(thd)_2$	$Se(SiEt_3)_2$, $Te(SiEt_3)_2$	170–210 (W)	0.25	[54]
$Li_3(BO_3)$-Li_2CO_3	LTB	O_3, TIB	200–260 (DT)	0.65	[211]

^{t}Bu: tert-butyl($(CH_3)_3C$-); Me: methyl(CH_3-); Et: Ethyl(CH_3CH_2-); Vi: vinyl(CH_2CH-); Am: amyl(C_5H_{11}-); ^{i}Pr: isopropyl($(CH_3)_2CH$-); Cp: cyclopentadienyl; Cyclotrisilazane: $(-NSiH_2)_3$; DMADMSE: 1,2-bis[(dimethylamino)dimethylsilyl]ethane 1,2-$[(NMe_2)Me_2Si]_2CH_2CH_2$; OMCTS: octamethylcyclotetrasiloxane $[(CH_3)_2SiO]_4$; TMS: trimethylsilane $(CH_3)_3SiH$; BDEAS: bis-diethylamino-silane ($(NEt_2)_2Si$); TDMAZr: tetrakis dimethylamino zirconium ($Zr[NEt_2]_4$); TBTDEN: (tert-butylimido)-tris(diethylamino)-niobium($(N^tBu)(Et_2N)_3Nb$; TMG: tris(dimethylamino)galium ($(NMe_2)_3Ga$); AMD: acetamidinato; thd: 2,2,6,6-tetramethyl-3,5-heptanedionate; acac: acetylacetonate; TDMAP: tris(dimethylamino)phosphine ($(NMe_2)_3PH_3$); HFAA: hexafluoroacetylacetone ($CF_3COCH_2COCF_3$); LTB: Lithium Tert-Butoxide (LiO^tBu); STB: Sodium Tert-Butoxide (NaO^tBu); dmamp: 2-Dimethylamino-2-methylpropanol ($(Me)_2C(CH_2OH)N(Me)_2$); TIB: triisopropyl borate $[(Me)_2CHO]_3B$.

alternating the deposition of Al_2O_3 followed by AlF_3 at 150 °C using trimethyl aluminum (TMA), H_2O, and HF as the reactants for aluminum, oxygen, and fluorine.[88]

3.2. Exchange Reaction Method

In the exchange reaction method, after the first ALD cycle, the other anion precursor is pulsed into the reaction chamber without the cation precursor pulse. This allows the exchange of anions from the already deposited ALD layer and the other anion precursor. Several mixed-anion ALD processes are using this approach.[31,89–92] Very recently Mahuli et al.[88] reported such a process for AlO_xF_y films based on HF fluorination of Al_2O_3. The process involves several cycles of Al_2O_3 followed by one or more HF pulses for the fluorination of the underlining Al_2O_3 layer. According to thermodynamics, the reaction of HF with Al_2O_3 produces AlF_3 along with the reaction, $Al_2O_3+6HF(g) \rightarrow AlF_3 + 3H_2O(g)$. Stoichiometry in the AlO_xF_y films is thus controlled by controlling the amount of HF pulsed in the reaction chamber.

3.3. Plasma-Enhanced ALD

Traditional ALD processes are based on temperature-induced reactions; they are sometimes called thermal-ALD processes. More recently, the research interest in plasma-enhanced (PE)-ALD is rapidly increasing, to expand the number and types of materials beyond the material set available to thermal-ALD. The technique has turned out to be highly useful in the field of mixed-anion thin films, in particular. In PE-ALD the same chemical precursors that are used in thermal-ALD processes are used, but the technique utilizes cycling of a radio frequency (RF)-plasma to complete the surface chemical reactions in a highly controlled manner. The technique retains the key benefits of the thermal-ALD, such as excellent conformality, thickness control, uniformity over the wafer, and fabricates the films at lower temperatures.

3.4. Spatial ALD

Spatial ALD (SALD) is a variation of ALD in which precursors are continuously supplied in different locations and kept separated by an inert gas region or zone. Film growth is achieved by exposing the substrate to the locations containing the different precursors. There are a few reports of mixed-anion SALD fabrications as well, for the fabrication of p-type Zn(O,N)[93–95] and the Zn(O,S) buffer layers for $Cu(In,Ga)Se_2$ solar cells.[96,97]

Besides the aforementioned four major approaches, there are also ALD processes for mixed-anion compounds in which the additional anion is simply brought to the film through one of the two main precursors; the examples include the process for the solid-electrolyte LiPON films where the phosphorus-containing anion precursor $PO(NH_2)(OEt)_2$ contains additionally both nitrogen and oxygen,[74] and the "unintentional" chlorine doping of TiO_2 films from the $TiCl_4$ cation precursor, appearing promising for Li^+-ion storage applications.[98]

4. State-of-the-Art Mixed-Anion ALD Thin Films

There are yet a very limited number of ALD processes developed for mixed-anion compounds, probably because of the paucity of suitable combinations of precursors with sufficient volatility and stability. The first report of ALD fabrication of a mixed-anion compound is from the year 1990 by Ozeki[19] for GaAs/GaP strained-layer superlattices. Later in 1992, Koukitu et al.[205] reported the epitaxial fabrication of Zn(S,Se) films, that is, an important material for blue light-emitting devices. They used Zn vapor, and H_2S and H_2Se gases as the source of zinc and the chalcogenides, respectively. For the last decade or so, the interest in the topic has experienced a significant boost, as was seen from Figure 2b.

4.1. Oxynitrides

The different oxynitrides have formed the major target in the ALD works so far reported for mixed-anion compounds. This is understandable considering their wide-range importance in electronics. Indeed, the fabrication of SiO_2, SiC, and Si_3N_4 thin films has represented a substantial segment of the ALD market, and there are no immediate reasons to believe that this situation would not continue in the future too. The aforementioned dielectric oxynitrides exhibit a range of useful optical, electronic, and barrier properties, and they moreover differ from each other in terms of the etch selectivity; hence, together they constitute an important material category for a wide variety of applications. Furthermore, these materials are essential building blocks for several ternary blends, such as silicon carboxides SiC_xO_y, silicon carbonitrides SiC_xN_y, and silicon oxynitrides SiO_xN_y, which also have unique applications in semiconductor manufacturing. For example, SiO_xN_y which is the intermediate between SiO_2 and Si_3N_4, possesses outstanding electronic and mechanical performance, such as low dielectric constant, high durability at high temperatures, and high resistance to thermal-shocks and oxidation.[212] Recently, Nishio et al.[213] predicted that the GaN/SiO_xN_y structure could be more stable than the SiO_2-terminated GaN/SiO_2 surface; this is very important for the creation of dangling-bond-free GaN/insulator interfaces.

Another exciting direction for the oxynitrides is seen in the various MPON-type metal phosphorus oxynitride electrolyte materials needed in the next-generation solid-state battery technologies. Indeed, highly promising ALD processes have already been reported for LiPON.[156–160] Similarly, phosphorus-free SnON[133] and TiON films have been investigated. Sowińska et al.[146] analyzed the effect of process parameters on the resultant oxygen-to-nitrogen ratio in their TiO_xN_y films fabricated by PE-ALD using either titanium isopropoxide and NH_3 plasma or tetrakis(dimethylamino)titanium and N_2 plasma as precursors. They observed that the O/N ratio had a huge impact on electrical properties such as conductivity and dielectric breakdown. Iwashita et al.[151] demonstrated thermal ALD combined with periodic oxidation for synthesizing TiO_xN_y films wherein oxygen was supplied periodically between the ALD-TiN cycles. Henkel et al.[147] observed bandgap narrowing in TiO_xN_y films with increasing nitrogen content due to the contribution of the nitrogen density of states.

Aluminum- and gallium-based oxynitride films have arisen some interest as well. Gallium oxynitride GaO_xN_y is an emerging material candidate for efficient heterostructures for photoelectrochemical (PEC) water splitting. In the PE-ALD process of Ma et al.[214] highly uniform GaO_xN_y films were obtained through a one-step co-deposition. The process enabled high-quality epitaxial growth of GaO_xN_y films on ZnO nanowires at 200 °C to construct ZnO/GaO_xN_y core-shell nanowires with different shell thicknesses (5–60 nm). Aluminum oxynitride AlO_xN_y films with different nitrogen contents have been deposited by thermal ALD on flexible nano-textured silicon surfaces for the surface passivation application.[138,139] The surfaces coated with AlO_xN_y films showed better surface recombination velocity due to the collective effect of field-effect passivation by the presence of fixed negative charges, and chemical passivation owing to hydrogen within the film.[137,138]

4.2. Carbonitrides

Transition-metal carbonitrides are the second most reported group of ALD-fabricated mixed-anion compounds. Compared to pure metals, binary transition-metal nitrides and carbides possess unique and useful property combinations, such as good metallic electrical conductivity and high resistance to heat and corrosion. Interest in the carbonitrides derives from the fact for these mixed-anion compounds even better physical properties may be achieved.[215,216] Transition-metal carbonitrides are often used as gate electrodes in high-k/metal gate transistors,[217,218] but many other fields such as thermodynamic[219] and catalytic[220] applications are emerging as well. Blakeney et al.[111] recently reported the ALD fabrication of titanium carbonitride TiC_xN_y thin films from $TiCl_4$ and aluminum dihydride complex, $AlH_2(^tBuNCH_2CH_2NMe_2)$, containing amido-amine ligands. The film growth proceeded via self-limited surface reactions with a high growth rate of 1.6–2.0 Å $cycle^{-1}$ within the appreciably wide deposition temperature window of 220–400 °C; the resultant films showed resistivity values around 600 µΩ-cm. Molybdenum carbonitride MoC_xN_y films were deposited through PE-ALD from $(^tBuN)_2(NMe_2)_2$ at temperatures ranging from 80 to 300 °C.[140] The composition, electrical properties, and optical properties are strongly dependent on the N_2/H_2 ratio in the gas stream, as well as the process.

Silicon carbonitride Si(C,N) is an intermediate phase between SiC and Si_3N_4, and has the added benefit of a lower dielectric constant than the parent phases, thus expanding the application potential from those typically reserved for Si_3N_4 or SiC. Ovanesyan et al.[100,221] developed a new ALD process for the fabrication of SiC_xN_y films using Si_2Cl_6 and CH_3NH_2 plasma as the sources for silicon and nitrogen, respectively. Under self-limiting growth conditions, the process led to highly conformal SiC_xN_y coatings on nanostructures with up to 9 at-% carbon composition. In the process, Si_2Cl_6 reacts primarily with the surface $-NH_2$ species created after the CH_3NH_2 plasma cycle. In the subsequent CH_3NH_2 half cycle, the surface chlorine is liberated, creating $-NH_x$ ($x = 1$ or 2) groups, and the carbon is incorporated primarily as $-N{=}C{=}N-$ species.

Tantalum carbonitrides TaC_xN_y films have been grown by PE-ALD from $Ta(N\text{-}t\text{-}C_5H_{11})[N(CH_3)_2]_3$ using H_2 or Ar/H_2 as the reducing agent.[106–108] The latter reducing agent appeared to break the Ta−N bond in the precursor to form TaC_x films; this resulted in the lower resistivity (≈255 µΩcm) compared with the case when H_2 was used as the reductant (≈1570 µΩcm).

4.3. Oxysulfides

Among the ALD-fabricated oxysulfide thin films, zinc oxysulfide Zn(O,S) is the most frequently reported material.[31,190,195,196,198,199,222–224] It is a wide bandgap semiconductor, for which the electronic and optical properties are controlled by the oxygen/sulfur content.[31,195,197,222,225,226] This makes it a potential candidate for buffer layers in thin-film photovoltaics.[227,228] Fine-tuning the sulfur content to obtain a slightly positive conduction band offset (≤0.5 eV)[195] and decreasing the buffer layer thickness[229,230] reduce the interfacial and bulk carrier recombination that allows for straightforward optimization of the PV cell performance.[199,223,231] The first ALD fabrication of Zn(O,S) films was reported in 1992, using dimethylzinc (DMZ), H_2O, and H_2S precursors.[198] Authors varied the sulfur content from 0 to 95% and observed a minimum in the bandgap and resistivity values around 60% sulfur content.

The same precursors, DMZ, H_2O, and H_2S, have been used in other studies as well. For example, Platzer-Björkman et al.[31] tailored the Zn(O,S) film composition systematically to use the films as buffer layers in $Cu(In,Ga)Se_2$ solar cells. Bakke et al.[199] controlled systematically the growth parameters, and observed a strong effect of the material properties on the optical characteristics of the Zn(O,S) films. The ALD growth and crystal structure of Zn(O,S) films resembled those of ZnS up to the ZnO/(ZnO+ZnS) cycle ratio of 0.6 with about 10% oxygen incorporated into the film. At higher cycle ratios the film structure became amorphous before recovering to crystalline films and the properties converge toward ALD-grown ZnO in terms of film growth rate, crystallinity, and composition. High-quality Zn(O,S) thin films can be grown from other precursors as well, for example, DEZ.[87,191]

Recently, thin MoO_xSe_y films (≈1–10 nm) were fabricated within TiO_2 nanotube layers and on sapphire substrates using $Mo(CO)_6$ and $(Me_3Si)_2Se$ precursors.[57] The $MoSe_xO_y$ coating enhanced significantly (four times) the incident photon-to-current conversion efficiency up to 32% (at $\lambda = 365$ nm), and also extended the photoresponse to the visible spectral region with a remarkable improvement of the photocurrent density up to ca. 40 times at $\lambda = 470$ nm. Another recent work reported the ALD fabrication of lanthanum copper oxysulfide LaOCuS films were deposited from $La(thd)_2$, ozone, $Cu(acac)_2$, and elemental sulfur; LaOCuS is a promising p-type thermoelectric material.[232]

4.4. Oxycarbides

Metal carbides, especially transition metal carbides, are frequently fabricated through ALD.[233–239] They have peculiar electronic properties,[239,240] and facilitate a broad range of promising applications in, for example, energy storage,[241] (electro)catalysis,[242] biosensing,[243] and biomedicine[244] through the synthesis of mixed-anion compounds such as SiO_xC_y. This compound is conventionally prepared by a so-called polymer-derived ceramic route via thermolysis of Si−C and Si−O containing polymer precursors (such as polysiloxanes and alkoxysilanes) in the inert gas atmosphere (Ar or N_2).[245,246] The method allows the incorporation of extra carbon into the SiO_xC_y network that inhibits high-temperature diffusion and crystallization of silicon, improving the high-temperature stability of SiO_xC_y.[247] In ALD literature, the silicon oxycarbide SiO_xC_y is also the most frequently reported mixed-anion carbide.[125–127,130,131,248] Recently, Closser et al.[125] fabricated SiO_xC_y films using bis(trichlorosilyl)methane and water as precursors at room temperature. They reported high-quality stable films with the following characteristics: density 1.4 g cm^{-3}, dielectric constant 2.6 ± 0.3, and refractive index 1.6 ± 0.1 at wavelength 633 nm, for potential applications for electronic devices. On the other hand, Zhou and Bent[127] fabricated SiO_xC_y from 1,2-bis[(dimethylamino)dimethylsilyl] ethane and ozone precursors. Here the problem was that the highly reactive ozone precursor tended to degrade the carbon within the film upon extended exposure.

4.5. Oxyfluorides

Two deposition pathways, the HF exchange method and the nanolaminate method, have been demonstrated for the growth of aluminum oxyfluoride AlO_xF_y films at 150 °C using TMA, water, and HF as precursors.[88] Linear AlO_xF_y growth was observed during both deposition methods and the compositional control was achieved either by changing the HF pressure during the HF exposure or by varying the thickness of the underlying Al_2O_3 layer before the HF exposure or by changing the ratio of the number of ALD Al_2O_3 and AlF_3 cycles.

5. Summary and Outlook

In this short review, we intended to summarize the current status of mixed-anion ALD and to provide some perspective for the potential applications of the ALD-grown mixed-anion thin films. As the ALD technique is becoming ubiquitous in many major fields of technology, the ALD fabrication of mixed-anion compounds may most likely become a true necessity as well. From the mixed-anion compounds' point of view, the ALD fabrication may be deemed necessary especially in applications where high-quality thin films on complex geometries and structures are required.

The metastability of many of the mixed-anion compounds as well as the high-temperature requirement for their synthesis using conventional techniques has been critical bottlenecks for the use of these materials in devices. The unique bottom-up and low-temperature fabrication by ALD could solve many of these problems and provide with us new approaches to manipulate the anion composition and the order/disorder. Several mixed-anion ALD processes have already shown the benefit, for example, the LiPON, SnON, and TiON thin films for solid-state battery technologies, where the O/N ratio has a huge impact on the actual device performance, for example, ionic conductivity and dielectric breakdown. Aluminum- and gallium-based oxynitride films have arisen considerable interest as well. The steadily increasing interest in ALD-fabricated mixed-anion compounds is expected to eventually lead us to new and improved material functionalities for many other applications as well, in catalysis, energy conversion, electronics, and beyond.

Most of the functional mixed-anion materials utilized to date are derived from metal oxides. In the future, the ALD approach could be extended to many other anions and their combinations, including even the organic molecular anions to complement the play with the presently employed inorganic anions mostly involving O, S, N, P, or Cl. Overall, with this wide palette of anions (based on abundant elements) we could design next-generation hybrid materials not only to address the inherent scarcity issues of metals but also to discover entirely new material functionalities. For the inclusion of organic molecular anions such as carboxylates (e.g., terephthalate), we like to emphasize the great potential provided by the currently strongly emerging ALD/MLD technique where ALD cycles are combined with MLD cycles for the organic constituent.[249–252] This could open completely new horizons for the entire field of mixed-anion compounds. There is still a lot to discover in the field of mixed-anion ALD, both for the scientific principles and technological applications, which indeed makes the field exciting and the prospects high.

Conflict of Interest

The authors declare no conflict of interest.

Keywords

atomic layer deposition, carbonitride, mixed-anion compound, oxyhalide, oxypnictide, oxysulfide, thin-film technology

Received: January 28, 2021
Revised: March 14, 2021

---

[1] H. Kageyama, K. Hayashi, K. Maeda, J. P. Attfield, Z. Hiroi, J. M. Rondinelli, K. R. Poeppelmeier, *Nat. Commun.* **2018**, *9*, 772.
[2] M. Yang, J. Oró-Solé, J. A. Rodgers, A. B. Jorge, A. Fuertes, J. P. Attfield, *Nat. Chem.* **2011**, *3*, 47.
[3] M. A. Hayward, *Science* **2002**, *295*, 1882.
[4] H. Hosono, K. Tanabe, E. Takayama-Muromachi, H. Kageyama, S. Yamanaka, H. Kumakura, M. Nohara, H. Hiramatsu, S. Fujitsu, *Sci. Technol. Adv. Mater.* **2015**, *16*, 033503.
[5] J. P. Attfield, *Cryst. Growth Des.* **2013**, *13*, 4623.
[6] H. Kageyama, T. Yajima, Y. Tsujimoto, T. Yamamoto, C. Tassel, Y. Kobayashi, *Bull. Chem. Soc. Jpn.* **2019**, *92*, 1349.
[7] G. Hitoki, T. Takata, J. N. Kondo, M. Hara, H. Kobayashi, K. Domen, *Chem. Commun.* **2002**, 1698.
[8] H. Fujito, H. Kunioku, D. Kato, H. Suzuki, M. Higashi, H. Kageyama, R. Abe, *J. Am. Chem. Soc.* **2016**, *138*, 2082.
[9] Y. Zhu, J. C. Gonzalez-Rosillo, M. Balaish, Z. D. Hood, K. J. Kim, J. L. M. Rupp, *Nat. Rev. Mater.* **2020**, https://doi.org/10.1038/s41578-020-00261-0.
[10] V. Lacivita, A. S. Westover, A. Kercher, N. D. Phillip, G. Yang, G. Veith, G. Ceder, N. J. Dudney, *J. Am. Chem. Soc.* **2018**, *140*, 11029.
[11] T. Ohno, L. Bai, T. Hisatomi, K. Maeda, K. Domen, *J. Am. Chem. Soc.* **2012**, *134*, 8254.
[12] L. D. Zhao, D. Berardan, Y. L. Pei, C. Byl, L. Pinsard-Gaudart, N. Dragoe, *Appl. Phys. Lett.* **2010**, *97*, 092118.
[13] L.-D. Zhao, J. He, D. Berardan, Y. Lin, J.-F. Li, C.-W. Nan, N. Dragoe, *Energy Env. Sci.* **2014**, *7*, 2900.
[14] Y. Pei, X. Shi, A. LaLonde, H. Wang, L. Chen, G. J. Snyder, *Nature* **2011**, *473*, 66.
[15] Y. Sadikin, M. Brighi, P. Schouwink, R. Černý, *Adv. Energy Mater.* **2015**, *5*, 1501016.
[16] N. P. Dasgupta, X. Meng, J. W. Elam, A. B. F. Martinson, *Acc. Chem. Res.* **2015**, *48*, 341.
[17] M. Leskelä, M. Mattinen, M. Ritala, *J. Vac. Sci. Technol., B* **2019**, *37*, 030801.
[18] X. Meng, Y.-C. Byun, H. Kim, J. Lee, A. Lucero, L. Cheng, J. Kim, *Materials* **2016**, *9*, 1007.
[19] M. Ozeki, *J. Vac. Sci. Technol., B* **1990**, *8*, 741.
[20] V. Vandalon, W. M. M. E. Kessels, *Langmuir* **2019**, *35*, 10374.

[21] C. S. Hwang, *Atomic Layer Deposition for Semiconductors*, Springer US, Boston, MA **2014**.

[22] *Atomic Layer Deposition of Nanostructured Materials*, (Eds. N. Pinna, M. Knez), Wiley-VCH, Weinheim **2012**.

[23] *Atomic Layer Deposition in Energy Conversion Applications*, (Ed. J. Bachmann), Wiley-VCH, Weinheim, Germany **2017**.

[24] N. K. R. Eswar, S. A. Singh, J. Heo, *J. Mater. Chem. A* **2019**, *7*, 17703.

[25] M.d. A. Hossain, K. T. Khoo, X. Cui, G. K. Poduval, T. Zhang, X. Li, W. M. Li, B. Hoex, *Nano Mater. Sci.* **2019**, *2*, 204.

[26] M. Leskelä, M. Ritala, *Angew. Chem., Int. Ed.* **2003**, *42*, 5548.

[27] S. M. George, *Chem. Rev.* **2010**, *110*, 111.

[28] J. Singh, S. Bent, C. E. D. Chidsey, M. W. Kanan, S. U. D. of Chemistry, *Nanomaterial Design Via ALD: New Methods and Applications in Catalysis*, Stanford University, Stanford, California, USA **2018**.

[29] T. Yoshimura, *Thin-Film Organic Photonics: Molecular Layer Deposition and Applications*, CRC Press/Taylor & Francis, Boca Raton, FL **2011**.

[30] M. Saadat, O. Amiri, A. Rahdar, *Sol. Energy* **2019**, *189*, 464.

[31] C. Platzer-Björkman, T. Törndahl, D. Abou-Ras, J. Malmström, J. Kessler, L. Stolt, *J. Appl. Phys.* **2006**, *100*, 044506.

[32] V. Miikkulainen, M. Leskelä, M. Ritala, R. L. Puurunen, *J. Appl. Phys.* **2013**, *113*, 021301.

[33] A. Hultqvist, M. Edoff, T. Törndahl, *Prog. Photovolt. Res. Appl.* **2011**, *19*, 478.

[34] A. Kosola, M. Putkonen, L.-S. Johansson, L. Niinistö, *Appl. Surf. Sci.* **2003**, *211*, 102.

[35] M. Vehkamäki, *Electrochem. Solid-State Lett.* **1999**, *2*, 504.

[36] H. Wang, J.-J. Wang, R. Gordon, J.-S. M. Lehn, H. Li, D. Hong, D. V. Shenai, *Electrochem. Solid-State Lett.* **2009**, *12*, G13.

[37] T. I. Hukka, R. E. Rawles, M. P. D'Evelyn, *Thin Solid Films* **1993**, *225*, 212.

[38] S. F. Komarov, J.-J. Lee, J. B. Hudson, M. P. D'Evelyn, *Diam. Relat. Mater.* **1998**, *7*, 1087.

[39] T. Choi, S. Yeo, J.-G. Song, S. Seo, B. Jang, S.-H. Kim, H. Kim, *Surf. Coat. Technol.* **2018**, *344*, 12.

[40] R. U. R. Sagar, X. Zhang, C. Xiong, Y. Yu, *Carbon* **2014**, *76*, 64.

[41] T. S. Tripathi, J. Lahtinen, M. Karppinen, *Adv. Mater. Interfaces* **2018**, *5*, 1701366.

[42] T. Suntola, J. Hyvarinen, *Annu. Rev. Mater. Sci.* **1985**, *15*, 177.

[43] J. T. Tanskanen, J. R. Bakke, S. F. Bent, T. A. Pakkanen, *Langmuir* **2010**, *26*, 11899.

[44] M. Włodarski, U. Chodorow, S. Jóźwiak, M. Putkonen, T. Durejko, T. Sajavaara, M. Norek, *Materials* **2019**, *12*, 3212.

[45] M. Z. Ansari, N. Parveen, D. K. Nandi, R. Ramesh, S. A. Ansari, T. Cheon, S.-H. Kim, *Sci. Rep.* **2019**, *9*, 10225.

[46] M. Pessa, R. Mäkelä, T. Suntola, *Appl. Phys. Lett.* **1981**, *38*, 131.

[47] B. Kalanyan, R. Beams, M. B. Katz, A. V. Davydov, J. E. Maslar, R. K. Kanjolia, *J. Vac. Sci. Technol., A* **2019**, *37*, 010901.

[48] H. Li, R. Zhao, J. Zhu, Z. Guo, W. Xiong, X. Wang, *Chem. Mater.* **2020**, *32*, 8885.

[49] M. Godlewski, E. Guziewicz, K. Kopalko, E. Łusakowska, E. Dynowska, M. M. Godlewski, E. M. Goldys, M. R. Phillips, *J. Lumin.* **2003**, *102–103*, 455.

[50] A. Yoshikawa, M. Kobayashi, S. Tokita, *Phys. Status Solidi B* **1995**, *187*, 315.

[51] M. Yokoyama, N. T. Chen, H. Y. Ueng, *J. Cryst. Growth* **2000**, *212*, 97.

[52] C. D. Lee, B. K. Kim, J. W. Kim, S. K. Chang, S. H. Suh, *J. Appl. Phys.* **1994**, *76*, 928.

[53] B. J. Choi, S. Choi, Y. C. Shin, K. M. Kim, C. S. Hwang, Y. J. Kim, Y. J. Son, S. K. Hong, *Chem. Mater.* **2007**, *19*, 4387.

[54] K. Zhang, A. D. R. Pillai, K. Bollenbach, D. Nminibapiel, W. Cao, H. Baumgart, T. Scherer, V. S. K. Chakravadhanula, C. Kübel, V. Kochergin, *ECS J. Solid State Sci. Technol.* **2014**, *3*, P207.

[55] V. Pore, T. Hatanpää, M. Ritala, M. Leskelä, *J. Am. Chem. Soc.* **2009**, *131*, 3478.

[56] T. Hatanpää, V. Pore, M. Ritala, M. Leskelä, *ECS Trans.* **2019**, *25*, 609.

[57] S. Ng, M. Krbal, R. Zazpe, J. Prikryl, J. Charvot, F. Dvořák, L. Strizik, S. Slang, H. Sopha, Y. Kosto, V. Matolin, F. K. Yam, F. Bures, J. M. Macak, *Adv. Mater. Interfaces* **2018**, *5*, 1701146.

[58] S. Yoo, C. Yoo, E.-S. Park, W. Kim, Y. K. Lee, C. S. Hwang, *J. Mater. Chem. C* **2018**, *6*, 5025.

[59] J. H. Jeong, D. J. Choi, *Mater. Sci. Semicond. Process.* **2016**, *54*, 42.

[60] H. Sopha, R. Zazpe, J. Prikryl, M. Krbal, S. Ng, F. Bures, J. M. Macak, *ECS Meet. Abstr.* **2020**, *MA2020-01*, 837.

[61] M. Ahonen, M. Pessa, T. Suntola, *Thin Solid Films* **1980**, *65*, 301.

[62] D.-W. Kim, J. Jang, H. Kim, K. Cho, S. Kim, *Thin Solid Films* **2008**, *516*, 7715.

[63] S. Song, D. Yao, Z. Song, L. Gao, Z. Zhang, L. Li, L. Shen, L. Wu, B. Liu, Y. Cheng, S. Feng, *Nanoscale Res. Lett.* **2015**, *10*, 89.

[64] M. Šilinskas, B. Kalkofen, R. Balasubramanian, A. Batmanov, E. P. Burte, N. Harmgarth, F. Zörner, F. T. Edelmann, B. Garke, M. Lisker, *J. Vac. Sci. Technol., A* **2018**, *36*, 021510.

[65] J. Hämäläinen, F. Munnik, M. Ritala, M. Leskelä, *Chem. Mater.* **2008**, *20*, 6840.

[66] T. Gwon, T. Eom, S. Yoo, C. Yoo, E. Park, S. Kim, M.-S. Kim, I. Buchanan, M. Xiao, S. Ivanov, C. S. Hwang, *Chem. Mater.* **2017**, *29*, 8065.

[67] T. Eom, S. Choi, B. J. Choi, M. H. Lee, T. Gwon, S. H. Rha, W. Lee, M.-S. Kim, M. Xiao, I. Buchanan, D.-Y. Cho, C. S. Hwang, *Chem. Mater.* **2012**, *24*, 2099.

[68] J. Dendooven, D. Deduytsche, J. Musschoot, R. L. Vanmeirhaeghe, C. Detavernier, *J. Electrochem. Soc.* **2010**, *157*, G111.

[69] H. B. Profijt, S. E. Potts, M. C. M. van de Sanden, W. M. M. Kessels, *J. Vac. Sci. Technol., A* **2011**, *29*, 050801.

[70] H. Kim, I.-K. Oh, *Jpn. J. Appl. Phys.* **2014**, *53*, 03DA01.

[71] S. M. Hwang, L. F. Peña, K. Tan, H. S. Kim, A. L. N. Kondusamy, Z. Qin, Y. C. Jung, J.-F. Veyan, D. Alvarez, J. Spiegelman, J. Kim, *ECS Trans.* **2019**, *92*, 265.

[72] S. Wolf, M. Edmonds, K. Sardashti, M. Clemons, J. H. Park, N. Yoshida, L. Dong, S. Nemani, E. Yieh, R. Holmes, D. Alvarez, A. C. Kummel, *Appl. Surf. Sci.* **2018**, *439*, 689.

[73] M. Juppo, M. Ritala, M. Leskelä, *J. Electrochem. Soc.* **2000**, *147*, 3377.

[74] M. Nisula, Y. Shindo, H. Koga, M. Karppinen, *Chem. Mater.* **2015**, *27*, 6987.

[75] A. V. Uvarov, A. S. Gudovskikh, *J. Phys.: Conf. Ser.* **2018**, *1038*, 012108.

[76] M. Ishii, S. Iwai, T. Ueki, Y. Aoyagi, *Thin Solid Films* **1998**, *318*, 6.

[77] M. Ishii, S. Iwai, T. Ueki, Y. Aoyagi, *Appl. Phys. Lett.* **1997**, *71*, 1044.

[78] Y. Yamamoto, R. Kurps, J. Murota, B. Tillack, *Solid-State Electron.* **2015**, *110*, 29.

[79] M. Ishizaki, N. Kano, J. Yoshino, H. Kukimoto, *Jpn. J. Appl. Phys.* **1991**, *30*, L428.

[80] D. Gu, D. Nminibapiel, H. Baumgart, H. Robinson, V. Kochergin, *ECS Transactions* **2011**, *41*, 255.

[81] Y. Lee, H. Sun, M. J. Young, S. M. George, *Chem. Mater.* **2016**, *28*, 2022.

[82] M. Ylilammi, *J. Electrochem. Soc.* **1994**, *141*, 1278.

[83] T. Pilvi, M. Ritala, M. Leskelä, M. Bischoff, U. Kaiser, N. Kaiser, *Appl. Opt.* **2008**, *47*, C271.

[84] Y. Lee, J. W. DuMont, A. S. Cavanagh, S. M. George, *J. Phys. Chem. C* **2015**, *119*, 14185.

[85] R. Heasley, C. M. Chang, L. M. Davis, K. Liu, R. G. Gordon, *J. Vac. Sci. Technol., A* **2017**, *35*, 01B109.

[86] G. Popov, M. Mattinen, T. Hatanpää, M. Vehkamäki, M. Kemell, K. Mizohata, J. Räisänen, M. Ritala, M. Leskelä, *Chem. Mater.* **2019**, *31*, 1101.

[87] S. Jeon, S. Bang, S. Lee, S. Kwon, W. Jeong, H. Jeon, H. J. Chang, H.-H. Park, *J. Korean Phys. Soc.* **2008**, *53*, 3287.
[88] N. Mahuli, A. S. Cavanagh, S. M. George, *J. Vac. Sci. Technol., A* **2020**, *38*, 022407.
[89] C. Bugot, N. Schneider, D. Lincot, F. Donsanti, *Beilstein J. Nanotechnol.* **2013**, *4*, 750.
[90] C. Bugot, N. Schneider, M. Bouttemy, A. Etcheberry, D. Lincot, F. Donsanti, *Thin Solid Films* **2015**, *582*, 340.
[91] P. Genevée, F. Donsanti, G. Renou, D. Lincot, *J. Phys. Chem. C* **2011**, *115*, 17197.
[92] M. Nakamura, Y. Kouji, Y. Chiba, H. Hakuma, T. Kobayashi, T. Nakada, in *2013 IEEE 39th Photovolt. Spec. Conf. PVSC*, IEEE, Tampa, FL, USA **2013**, pp. 0849–0852.
[93] L. Dunlop, A. Kursumovic, J. L. MacManus-Driscoll, *Appl. Phys. Lett.* **2008**, *93*, 172111.
[94] B. Ehrler, K. P. Musselman, M. L. Böhm, F. S. F. Morgenstern, Y. Vaynzof, B. J. Walker, J. L. MacManus-Driscoll, N. C. Greenham, *ACS Nano* **2013**, *7*, 4210.
[95] K. P. Musselman, S. Albert-Seifried, R. L. Z. Hoye, A. Sadhanala, D. Muñoz-Rojas, J. L. MacManus-Driscoll, R. H. Friend, *Adv. Funct. Mater.* **2014**, *24*, 3562.
[96] C. H. Frijters, P. Poodt, A. Illiberi, *Sol. Energy Mater. Sol. Cells* **2016**, *155*, 356.
[97] A. Illiberi, C. Frijters, M. Ruth, D. Bremaud, P. Poodt, F. Roozeboom, P. J. Bolt, *J. Vac. Sci. Technol., A* **2018**, *36*, 051511.
[98] S. Moitzheim, J. E. Balder, P. Poodt, S. Unnikrishnan, S. De Gendt, P. M. Vereecken, *Chem. Mater.* **2017**, *29*, 10007.
[99] A. Bertuch, B. D. Keller, N. Ferralis, J. C. Grossman, G. Sundaram, *J. Vac. Sci. Technol., A* **2017**, *35*, 01B141.
[100] R. A. Ovanesyan, N. Leick, K. M. Kelchner, D. M. Hausmann, S. Agarwal, *Chem. Mater.* **2017**, *29*, 6269.
[101] Y.-L. Hsu, Y.-F. Chang, W.-M. Chung, Y.-C. Chen, C.-C. Lin, J. Leu, *Appl. Phys. Lett.* **2020**, *116*, 213502.
[102] A. Abdelal, Z. Khatami, P. Mascher, *ECS Trans.* **2020**, *97*, 59.
[103] J. Goff, C. M. Brick, A. Kaloyeros, B. Arkles, *ECS Trans.* **2020**, *98*, 121.
[104] G. Cho, S.-W. Rhee, *Electrochem. Solid-State Lett.* **2010**, *13*, H426.
[105] S.-H. Kim, M.-K. Song, S.-W. Rhee, *J. Electrochem. Soc.* **2010**, *157*, H652.
[106] M.-K. Song, S. Rhee, *J. Electrochem. Soc.* **2008**, *155*, H823.
[107] C. Hossbach, S. Teichert, J. Thomas, L. Wilde, H. Wojcik, D. Schmidt, B. Adolphi, M. Bertram, U. Mühle, M. Albert, S. Menzel, B. Hintze, J. W. Bartha, *J. Electrochem. Soc.* **2009**, *156*, H852.
[108] T. J. Park, J. H. Kim, J. H. Jang, K. D. Na, C. S. Hwang, J. H. Kim, G.-M. Kim, J. H. Choi, K. J. Choi, J. H. Jeong, *Appl. Phys. Lett.* **2007**, *91*, 252106.
[109] P. Alén, M. Juppo, M. Ritala, T. Sajavaara, J. Keinonen, M. Leskelä, *J. Electrochem. Soc.* **2001**, *148*, G566.
[110] G. Cho, S.-W. Rhee, *ECS J. Solid State Sci. Technol.* **2014**, *3*, P185.
[111] K. J. Blakeney, P. D. Martin, C. H. Winter, *Dalt. Trans.* **2018**, *47*, 10897.
[112] W. Zeng, X. Wang, S. Kumar, D. W. Peters, E. T. Eisenbraun, *J. Mater. Res.* **2007**, *22*, 703.
[113] H. Kim, J. Park, H. Jeon, W. Jang, H. Jeon, J. Yuh, *J. Vac. Sci. Technol., A* **2015**, *33*, 05E111.
[114] H. Kim, W. Jang, C. Shin, K. Lee, H. Lim, M. Kim, J. Yuh, H. Jeon, *Phys. Status Solidi A* **2017**, *214*, 1700010.
[115] W. Besling, A. S. Satta, J. Schuhmacher, T. Abell, V. Sutcliffe, A.-M. Hoyas, G. Beyer, D. Gravesteijn, K. Maex, in *Proc. IEEE 2002 Int. Interconnect Technol. Conf. Cat No02EX519*, IEEE, Burlingame, CA, USA **2002**, pp. 288–291.
[116] K.-E. Elers, V. Saanila, W.-M. Li, P. J. Soininen, J. T. Kostamo, S. Haukka, J. Juhanoja, W. F. A. Besling, *Thin Solid Films* **2003**, *434*, 94.
[117] A. M. Hoyas, J. Schuhmacher, D. Shamiryan, J. Waeterloos, W. Besling, J. P. Celis, K. Maex, *J. Appl. Phys.* **2004**, *95*, 381.
[118] Y. Travaly, J. Schuhmacher, A. M. Hoyas, M. Van Hove, K. Maex, T. Abell, V. Sutcliffe, A. M. Jonas, *J. Appl. Phys.* **2005**, *97*, 084316.
[119] A. M. Hoyas, J. Schuhmacher, C. M. Whelan, T. Fernandez Landaluce, D. Vanhaeren, K. Maex, J. P. Celis, *J. Appl. Phys.* **2006**, *100*, 114903.
[120] A. M. Hoyas, J. Schuhmacher, C. M. Whelan, T. Fernandez Landaluce, D. Vanhaeren, K. Maex, J. P. Celis, *J. Appl. Phys.* **2006**, *100*, 114903.
[121] H. Volders, Z. Tökei, H. Bender, B. Brijs, R. Caluwaerts, L. Carbonell, T. Conard, C. Drijbooms, A. Franquet, S. Garaud, I. Hoflijk, A. Moussa, F. Sinapi, Y. Travaly, D. Vanhaeren, G. Vereecke, C. Zhao, W.-M. Li, H. Sprey, A. M. Jonas, *Microelectron. Eng.* **2007**, *84*, 2460.
[122] S. Y. Lee, B.-K. Ju, Y. T. Kim, *Jpn. J. Appl. Phys.* **2018**, *57*, 04FC01.
[123] T. Muneshwar, K. Cadien, *Appl. Surf. Sci.* **2018**, *435*, 367.
[124] A. Ul-Hamid, *Mater. Adv.* **2020**, *1*, 988.
[125] R. G. Closser, D. S. Bergsman, S. F. Bent, *ACS Appl. Mater. Interfaces* **2018**, *10*, 24266.
[126] M. Arango-Ospina, F. Xie, I. Gonzalo-Juan, R. Riedel, E. Ionescu, A. R. Boccaccini, *Appl. Mater. Today* **2020**, *18*, 100482.
[127] H. Zhou, S. F. Bent, *J. Phys. Chem. C* **2013**, *117*, 19967.
[128] J. B. Bhaskar, M. Saly, Methods for Atomic Layer Deposition of SiCO(N) Using Halogenated Silylamides, US patent, Application number: US20200010954A1, January **2020**.
[129] M. Wang, H. Chandra, X. Lei, A. Mallikarjunan, K. Cuthill, M. Xiao, *J. Vac. Sci. Technol., A* **2018**, *36*, 021509.
[130] J. Lee, W. Jang, H. Kim, S. Shin, Y. Kweon, K. Lee, H. Jeon, *Thin Solid Films* **2018**, *645*, 334.
[131] K.-M. Lee, C. Y. Kim, C. K. Choi, R. Navamathavan, J. Kor, *Phys. Soc.* **2011**, *59*, 3074.
[132] S. Suh, S. W. Ryu, S. Cho, J.-R. Kim, S. Kim, C. S. Hwang, H. J. Kim, *J. Vac. Sci. Technol., A* **2016**, *34*, 01A136.
[133] D. M. Stewart, A. J. Pearse, N. S. Kim, E. J. Fuller, A. A. Talin, K. Gregorczyk, S. B. Lee, G. W. Rubloff, *Chem. Mater.* **2018**, *30*, 2526.
[134] M.-C. Tsai, M.-H. Lee, C.-L. Kuo, H.-C. Lin, M.-J. Chen, *Appl. Surf. Sci.* **2016**, *387*, 274.
[135] A. W. Amer, M. A. El-Sayed, N. K. Allam, *J. Phys. Chem. C* **2016**, *120*, 7025.
[136] M. Ziegler, S. Linzen, S. Goerke, U. Bruckner, J. Plentz, J. Dellith, A. Himmerlich, M. Himmerlich, U. Hubner, S. Krischok, H.-G. Meyer, *IEEE Trans. Appl. Supercond.* **2017**, *27*, 1.
[137] A. I. Abdulagatov, R. R. Amashaev, K.r. N. Ashurbekova, K. N. Ashurbekova, M. Kh. Rabadanov, I. M. Abdulagatov, *Russ. J. Gen. Chem.* **2018**, *88*, 1699.
[138] P. K. Parashar, S. A. Kinnunen, T. Sajavaara, J. J. Toppari, V. K. Komarala, *Sol. Energy Mater. Sol. Cells* **2019**, *193*, 231.
[139] H.-Y. Chen, H.-L. Lu, J.-X. Chen, F. Zhang, X.-M. Ji, W.-J. Liu, X.-F. Yang, D. W. Zhang, *ACS Appl. Mater. Interfaces* **2017**, *9*, 38662.
[140] M. Nozaki, K. Watanabe, T. Yamada, H.-A. Shih, S. Nakazawa, Y. Anda, T. Ueda, A. Yoshigoe, T. Hosoi, T. Shimura, H. Watanabe, *Jpn. J. Appl. Phys.* **2018**, *57*, 06KA02.
[141] S.-K. Eom, M.-W. Kong, H.-Y. Cha, K.-S. Seo, *IEEE J. Electron Devices Soc.* **2019**, *7*, 908.
[142] J.-Y. Wu, Y.-T. Chen, M.-H. Lin, T.-B. Wu, *IEEE Electron Device Lett.* **2010**, *31*, 993.
[143] S. Kim, J. Y. Kim, J. Kim, J. Choi, H. Kang, C. Bae, H. Jeon, *Electrochem. Solid-State Lett.* **2006**, *9*, G40.
[144] H.-P. Ma, J.-H. Yang, J.-J. Tao, K.-P. Yuan, P.-H. Cheng, W. Huang, J.-C. Wang, Q.-X. Guo, H.-L. Lu, D. W. Zhang, *Nano Energy* **2019**, *66*, 104089.
[145] H.-P. Ma, X.-X. Li, J.-H. Yang, P. Cheng, W. Huang, J. Zhu, T.-C. Jen, Q. Guo, H.-L. Lu, D. W. Zhang, *Chem. Mater.* **2019**, *31*, 7405.

[146] M. Sowińska, S. Brizzi, C. Das, I. Kärkkänen, J. Schneidewind, F. Naumann, H. Gargouri, K. Henkel, D. Schmeißer, *Appl. Surf. Sci.* **2016**, *381*, 42.
[147] K. Henkel, C. Das, M. Kot, D. Schmeißer, F. Naumann, I. Kärkkänen, H. Gargouri, *J. Vac. Sci. Technol., A* **2017**, *35*, 01B135.
[148] M. Sowińska, K. Henkel, D. Schmeißer, I. Kärkkänen, J. Schneidewind, F. Naumann, B. Gruska, H. Gargouri, *J. Vac. Sci. Technol., A* **2016**, *34*, 01A127.
[149] M. Kot, K. Henkel, C. Das, S. Brizzi, I. Kärkkänen, J. Schneidewind, F. Naumann, H. Gargouri, D. Schmeißer, *Surf. Coat. Technol.* **2017**, *324*, 586.
[150] G. K. Hyde, S. D. McCullen, S. Jeon, S. M. Stewart, H. Jeon, E. G. Loboa, G. N. Parsons, *Biomed. Mater.* **2009**, *4*, 025001.
[151] S. Iwashita, S. Aoyama, M. Nasu, K. Shimomura, N. Noro, T. Hasegawa, Y. Akasaka, K. Miyashita, *J. Vac. Sci. Technol., A* **2016**, *34*, 01A145.
[152] Y. Gao, J. Park, X. Liang, *J. Electrochem. Soc.* **2018**, *165*, A3871.
[153] Y.-Q. Cao, X.-R. Zhao, J. Chen, W. Zhang, M. Li, L. Zhu, X.-J. Zhang, D. Wu, A.-D. Li, *Sci. Rep.* **2018**, *8*, 12131.
[154] A. Lee, J. A. Libera, R. Z. Waldman, A. Ahmed, J. R. Avila, J. W. Elam, S. B. Darling, *Adv. Sustainable Syst.* **2017**, *1*, 1600041.
[155] E.-J. Song, H. Jo, S.-H. Kwon, J.-H. Ahn, J.-D. Kwon, *Thin Solid Films* **2020**, *694*, 137752.
[156] A. C. Kozen, A. J. Pearse, C.-F. Lin, M. Noked, G. W. Rubloff, *Chem. Mater.* **2015**, *27*, 5324.
[157] B. Put, M. J. Mees, N. Hornsveld, S. Hollevoet, A. Sepúlveda, P. M. Vereecken, W. M. M. Kessels, M. Creatore, *J. Electrochem. Soc.* **2019**, *166*, A1239.
[158] C.-F. Lin, X. Fan, A. Pearse, S.-C. Liou, K. Gregorczyk, M. Leskes, C. Wang, S. B. Lee, G. W. Rubloff, M. Noked, *Chem. Mater.* **2017**, *29*, 8780.
[159] S. Shibata, *J. Electrochem. Soc.* **2016**, *163*, A2555.
[160] A. J. Pearse, T. E. Schmitt, E. J. Fuller, F. El-Gabaly, C.-F. Lin, K. Gerasopoulos, A. C. Kozen, A. A. Talin, G. Rubloff, K. E. Gregorczyk, *Chem. Mater.* **2017**, *29*, 3740.
[161] R. B. Nuwayhid, A. Jarry, G. W. Rubloff, K. E. Gregorczyk, *ACS Appl. Mater. Interfaces* **2020**, *12*, 21641.
[162] A. R. Mouat, A. U. Mane, J. W. Elam, M. Delferro, T. J. Marks, P. C. Stair, *Chem. Mater.* **2016**, *28*, 1907.
[163] A. Dhara, D. Saha, S. Mitra, S. K. Sarkar, *J. Vac. Sci. Technol., A* **2020**, *38*, 022409.
[164] Y.-P. Wang, X. Wu, W.-J. Liu, D. W. Zhang, S.-J. Ding, *ACS Appl. Electron. Mater.* **2020**, *2*, 1653.
[165] T. Sugawara, Y. Oshima, R. Sreenivasan, P. C. McIntyre, *Appl. Phys. Lett.* **2007**, *90*, 112912.
[166] M. Ritala, P. Kalsi, D. Riihelä, K. Kukli, M. Leskelä, J. Jokinen, *Chem. Mater.* **1999**, *11*, 1712.
[167] H. Hajibabaei, O. Zandi, T. W. Hamann, *Chem. Sci.* **2016**, *7*, 6760.
[168] Z. Ma, K. Piętak, J. Piątek, J. R. DeMoulpied, A. Rokicińska, P. Kuśtrowski, R. Dronskowski, S. Zlotnik, R. H. Coridan, A. Slabon, *Chem. Commun.* **2020**, *56*, 13193.
[169] C. Lee, J. Lim, *J. Vac. Sci. Technol., A* **2006**, *24*, 1031.
[170] D. Garcia-Alonso, S. E. Potts, C. A. A. van Helvoirt, M. A. Verheijen, W. M. M. Kessels, *J. Mater. Chem. C* **2015**, *3*, 3095.
[171] A. Yamada, B. Sang, M. Konagai, *Appl. Surf. Sci.* **1997**, *112*, 216.
[172] T. Tynell, R. Okazaki, I. Terasaki, H. Yamauchi, M. Karppinen, *J. Mater. Sci.* **2013**, *48*, 2806.
[173] H. Yuan, B. Luo, S. A. Campbell, W. L. Gladfelter, *Electrochem. Solid-State Lett.* **2011**, *14*, H181.
[174] M. Tiitta, E. Nykänen, P. Soininen, L. Niinistö, M. Leskelä, R. Lappalainen, *Mater. Res. Bull.* **1998**, *33*, 1315.
[175] M. Nieminen, L. Niinistö, R. Lappalainen, *Microchim. Acta* **1995**, *119*, 13.
[176] J. Liu, Y. Tang, B. Xiao, T.-K. Sham, R. Li, X. Sun, *RSC Adv.* **2013**, *3*, 4492.
[177] S. Knohl, A. K. Roy, R. Lungwitz, S. Spange, T. Mäder, D. J. Nestler, B. Wielage, S. Schulze, M. Hietschold, H. Wulff, C. A. Helm, F. Seidel, D. R. T. Zahn, W. A. Goedel, *ACS Appl. Mater. Interfaces* **2013**, *5*, 6161.
[178] T. Dobbelaere, A. K. Roy, P. Vereecken, C. Detavernier, *Chem. Mater.* **2014**, *26*, 6863.
[179] V. E. Strempel, D. Löffler, J. Kröhnert, K. Skorupska, B. Johnson, R. N. d'Alnoncourt, M. Driess, F. Rosowski, *J. Vac. Sci. Technol., A* **2016**, *34*, 01A135.
[180] B. Xiao, B. Wang, J. Liu, K. Kaliyappan, Q. Sun, Y. Liu, G. Dadheech, M. P. Balogh, L. Yang, T.-K. Sham, R. Li, M. Cai, X. Sun, *Nano Energy* **2017**, *34*, 120.
[181] N. Hornsveld, W. M. M. Kessels, M. Creatore, *J. Phys. Chem. C* **2020**, *124*, 5495.
[182] M. Putkonen, T. Sajavaara, P. Rahkila, L. Xu, S. Cheng, L. Niinistö, H. J. Whitlow, *Thin Solid Films* **2009**, *517*, 5819.
[183] J. Su, T. Tsuruoka, T. Tsujita, Y. Nishitani, K. Nakura, K. Terabe, *Chem. Mater.* **2019**, *31*, 5566.
[184] S. W. Park, D. Y. Jang, J. W. Kim, J. H. Shim, *J. Vac. Sci. Technol., A* **2015**, *33*, 041511.
[185] O. Tiurin, N. Solomatin, M. Auinat, Y. Ein-Eli, *J. Power Sources* **2020**, *448*, 227373.
[186] Y.-J. Choi, H.-H. Park, *J. Mater. Chem. C* **2014**, *2*, 98.
[187] K. Kukli, M. Mikkor, A. Šutka, M. Kull, H. Seemen, J. Link, R. Stern, A. Tamm, *J. Magn. Magn. Mater.* **2020**, *498*, 166167.
[188] D. Riihelä, M. Ritala, R. Matero, M. Leskelä, *Thin Solid Films* **1996**, *289*, 250.
[189] C. Bugot, N. Schneider, D. Lincot, F. Donsanti, *J. Appl. Phys.* **2018**, *123*, 185306.
[190] A. L. Dadlani, S. Acharya, O. Trejo, F. B. Prinz, J. Torgersen, *ACS Appl. Mater. Interfaces* **2016**, *8*, 14323.
[191] E. B. Yousfi, T. Asikainen, V. Pietu, P. Cowache, M. Powalla, D. Lincot, *Thin Solid Films* **2000**, *361–362*, 183.
[192] T. Törndahl, A. Hultqvist, C. Platzer-Björkman, M. Edoff, *Proceedings of SPIE* **2010**, *7603*, 76030D-1.
[193] C. Bugot, N. Schneider, M. Jubault, D. Lincot, F. Donsanti, *J. Vac. Sci. Technol., A* **2015**, *33*, 01A151.
[194] D. K. Lancaster, H. Sun, S. M. George, *J. Phys. Chem. C* **2017**, *121*, 18643.
[195] G.-R. Uhm, S. Y. Jang, Y. H. Jeon, H. K. Yoon, H. Seo, *RSC Adv.* **2014**, *4*, 28111.
[196] W.-J. Choi, W. W. Park, Y. Kim, C. S. Son, D. Hwang, *Energies* **2020**, *13*, 412.
[197] K. Ramanathan, J. Mann, S. Glynn, S. Christensen, J. Pankow, J. Li, J. Scharf, L. Mansfield, M. Contreras, R. Noufi, in *2012 38th IEEE Photovolt. Spec. Conf.*, IEEE, Austin, TX, USA **2012**, pp. 001677–001681.
[198] B. W. Sanders, A. Kitai, *Chem. Mater.* **1992**, *4*, 1005.
[199] J. R. Bakke, J. T. Tanskanen, C. Hägglund, T. A. Pakkanen, S. F. Bent, *J. Vac. Sci. Technol., A* **2012**, *30*, 01A135.
[200] K. Kukli, M. Peussa, L.-S. Johansson, E. Nykänen, L. Niinistö, *Mater. Sci. Forum* **1999**, *315–317*, 216.
[201] J. Rosa, J. Deuermeier, P. J. Soininen, M. Bosund, Z. Zhu, E. Fortunato, R. Martins, M. Sugiyama, S. Merdes, *Materials* **2019**, *13*, 93.
[202] C. Schwartz, D. Nordlund, T.-C. Weng, D. Sokaras, L. Mansfield, A. S. Krishnapriyan, K. Ramanathan, K. E. Hurst, D. Prendergast, S. T. Christensen, *Sol. Energy Mater. Sol. Cells* **2016**, *149*, 275.
[203] C. Bugot, M. Bouttemy, N. Schneider, A. Etcheberry, D. Lincot, F. Donsanti, *J. Vac. Sci. Technol., A* **2018**, *36*, 061510.
[204] J.-W. Choi, J. Oh, T. T. Ngoc Van, J. Kim, H. Hwang, C. G. Kim, T.-M. Chung, K.-S. An, B. Shong, J.-H. Hwang, *Ceram. Int.* **2020**, *46*, 5109.

[205] A. Koukitu, H. Ikeda, T. Miyazawa, H. Seki, *Jpn. J. Appl. Phys.* **1992**, *31*, L1463.
[206] J. Ihanus, E. Lambers, P. H. Holloway, M. Ritala, M. Leskelä, *J. Cryst. Growth* **2004**, *260*, 440.
[207] C. T. Hsu, *Mater. Chem. Phys.* **1999**, *58*, 6.
[208] N.-T. Chen, M. Yokoyama, H.-Y. Ueng, *J. Cryst. Growth* **2000**, *216*, 152.
[209] J. Lee, S. Choi, C. Lee, Y. Kang, D. Kim, *Appl. Surf. Sci.* **2007**, *253*, 3969.
[210] Y. K. Ezhovskii, *Russ. J. Phys. Chem. A* **2014**, *88*, 1580.
[211] E. Kazyak, K.-H. Chen, A. L. Davis, S. Yu, A. J. Sanchez, J. Lasso, A. R. Bielinski, T. Thompson, J. Sakamoto, D. J. Siegel, N. P. Dasgupta, *J. Mater. Chem. A* **2018**, *6*, 19425.
[212] Y. Shi, L. He, F. Guang, L. Li, Z. Xin, R. Liu, *Micromachines* **2019**, *10*, 552.
[213] K. Nishio, T. Yayama, T. Miyazaki, N. Taoka, M. Shimizu, *Sci. Rep.* **2018**, *8*, 1391.
[214] H.-P. Ma, J.-H. Yang, J.-J. Tao, K.-P. Yuan, P.-H. Cheng, W. Huang, J.-C. Wang, Q.-X. Guo, H.-L. Lu, D. W. Zhang, *Nano Energy* **2019**, *66*, 104089.
[215] M. Yoshitake, *J. Vac. Sci. Technol., A* **2014**, *32*, 061403.
[216] H. Kim, *J. Vac. Sci. Technol., B* **2003**, *21*, 2231.
[217] T. J. Park, J. H. Kim, J. H. Jang, K. D. Na, C. S. Hwang, G.-M. Kim, K. J. Choi, J. H. Jeong, *Appl. Phys. Lett.* **2008**, *92*, 202902.
[218] M. Kadoshima, K. Akiyama, K. Yamamoto, H. Fujiwara, T. Yasuda, T. Nabatame, A. Toriumi, *J. Vac. Sci. Technol., B* **2005**, *23*, 42.
[219] S. K. Gupta, S. D. Gupta, H. R. Soni, V. Mankad, P. K. Jha, *Mater. Chem. Phys.* **2014**, *143*, 503.
[220] E. F. de Souza, T. C. Ramalho, C. A. Chagas, R. B. de Alencastro, *Catal. Sci. Technol.* **2014**, *4*, 2550.
[221] R. A. Ovanesyan, E. A. Filatova, S. D. Elliott, D. M. Hausmann, D. C. Smith, S. Agarwal, *J. Vac. Sci. Technol., A* **2019**, *37*, 060904.
[222] S. Sinha, H. V. Ramasamy, D. K. Nandi, P. N. Didwal, J. Y. Cho, C.-J. Park, Y.-S. Lee, S.-H. Kim, J. Heo, *J. Mater. Chem. A* **2018**, *6*, 16515.
[223] B. K. Meyer, A. Polity, B. Farangis, Y. He, D. Hasselkamp, Th. Krämer, C. Wang, *Appl. Phys. Lett.* **2004**, *85*, 4929.
[224] H. K. Hong, I. Y. Kim, S. W. Shin, G. Y. Song, J. Y. Cho, M. G. Gang, J. C. Shin, J. H. Kim, J. Heo, *Sol. Energy Mater. Sol. Cells* **2016**, *155*, 43.
[225] T. Minemoto, A. Okamoto, H. Takakura, *Thin Solid Films* **2011**, *519*, 7568.
[226] R. R. Thankalekshmi, A. C. Rastogi, *J. Appl. Phys.* **2012**, *112*, 063708.
[227] R. L. Garris, J. V. Li, M. A. Contreras, K. Ramanathan, L. M. Mansfield, B. Egaas, A. Kanevce, in *2014 IEEE 40th Photovolt. Spec. Conf. PVSC*, IEEE, Denver, CO, USA **2014**, pp. 0353–0356.
[228] K. X. Steirer, R. L. Garris, J. V. Li, M. J. Dzara, P. F. Ndione, K. Ramanathan, I. Repins, G. Teeter, C. L. Perkins, *Phys. Chem. Chem. Phys.* **2015**, *17*, 15355.
[229] A. Chihi, M. F. Boujmil, B. Bessais, *Int. J. Phys. Sci.* **2014**, *9*, 250.
[230] J. Sun, V. Nalla, M. Nguyen, Y. Ren, S. Y. Chiam, Y. Wang, K. F. Tai, H. Sun, N. Zheludev, S. K. Batabyal, L. H. Wong, *Sol. Energy* **2015**, *115*, 396.
[231] A. L. Dadlani, O. Trejo, S. Acharya, J. Torgersen, I. Petousis, D. Nordlund, R. Sarangi, P. Schindler, F. B. Prinz, *J. Mater. Chem. C* **2015**, *3*, 12192.
[232] A. Matikainen, *Mixed-Anion Compounds: An Unexplored ALD Playground for Applications, Thesis*, Aalto University, Finland **2018**.
[233] M. Sarr, N. Bahlawane, D. Arl, M. Dossot, E. McRae, D. Lenoble, *J. Phys. Chem. C* **2014**, *118*, 23385.
[234] M. Sarr, N. Bahlawane, D. Arl, M. Dossot, E. McRae, D. Lenoble, *Appl. Surf. Sci.* **2016**, *379*, 523.
[235] J. Moon, H. J. Ahn, Y. Seo, T. I. Lee, C.-K. Kim, I. C. Rho, C. H. Kim, W. S. Hwang, B. J. Cho, *IEEE Trans. Electron Devices* **2016**, *63*, 1423.
[236] H. J. Ahn, J. Moon, S. Koh, Y. Seo, C.-K. Kim, I. C. Rho, C. H. Kim, W. S. Hwang, B. J. Cho, *IEEE Trans. Electron Devices* **2016**, *63*, 2858.
[237] S. Kim, D. Geum, S. K. Kim, H. Kim, J. D. Song, W. J. Choi, in *2016 IEEE SOI-3D-Subthreshold Microelectron. Technol. Unified Conf. S3S*, IEEE, Burlingame, CA, USA **2016**, pp. 1–2.
[238] J. B. Kim, S.-H. Kim, W. S. Han, D.-J. Lee, *J. Vac. Sci. Technol., A* **2016**, *34*, 041504.
[239] H. H. Hwu, J. G. Chen, *Chem. Rev.* **2005**, *105*, 185.
[240] Y. Gogotsi, *Nat. Mater.* **2015**, *14*, 1079.
[241] B. Anasori, M. R. Lukatskaya, Y. Gogotsi, *Nat. Rev. Mater.* **2017**, *2*, 16098.
[242] W. Wan, B. M. Tackett, J. G. Chen, *Chem. Soc. Rev.* **2017**, *46*, 1807.
[243] B. Xu, M. Zhu, W. Zhang, X. Zhen, Z. Pei, Q. Xue, C. Zhi, P. Shi, *Adv. Mater.* **2016**, *28*, 3333.
[244] J. Yu, C. Yang, J. Li, Y. Ding, L. Zhang, M. Z. Yousaf, J. Lin, R. Pang, L. Wei, L. Xu, F. Sheng, C. Li, G. Li, L. Zhao, Y. Hou, *Adv. Mater.* **2014**, *26*, 4114.
[245] P. Colombo, G. Mera, R. Riedel, G. D. Sorarù, *J. Am. Ceram. Soc.* **2010**, *93*, 1805.
[246] R. Riedel, G. Mera, R. Hauser, A. Klonczynski, *J. Ceram. Soc. Jpn.* **2006**, *114*, 425.
[247] A. Saha, R. Raj, D. L. Williamson, *J. Am. Ceram. Soc.* **2006**, *89*, 2188.
[248] Y.-B. Jiang, N. Liu, H. Gerung, J. L. Cecchi, C. J. Brinker, *J. Am. Chem. Soc.* **2006**, *128*, 11018.
[249] A. J. Karttunen, T. Tynell, M. Karppinen, *J. Phys. Chem. C* **2015**, *119*, 13105.
[250] M. Nisula, M. Karppinen, *Nano Lett.* **2016**, *16*, 1276.
[251] R. Ghiyasi, G. C. Tewari, M. Karppinen, *J. Phys. Chem. C* **2020**, *124*, 13765.
[252] A. Khayyami, A. Philip, J. Multia, M. Karppinen, *Dalt. Trans.* **2020**, *49*, 11310.

Tripurari Sharan Tripathi is a postdoctoral researcher at the School of Science, Aalto University, Finland. He received his Ph.D. degree in physics at JNU, India in 2012 for works on electronic transport and magnetic properties of chromium chalcogenide spinels, known for their room-temperature ferromagnetic and metallic properties. Subsequently, he worked at the NUS, Singapore, and IUAC, India as a postdoc researcher on oxide and chalcogenide materials for magnetic and thermoelectric applications. Currently, he is working on semiconductor devices and using ALD and other surface passivation techniques to enhance the efficiency of the devices.

Maarit Karppinen is a distinguished professor in Inorganic Materials Chemistry at Aalto University, Finland, since 2006. Before that she had professor chair at Tokyo Institute of Technology, Japan. Her interdisciplinary research is focused on new functional materials for various emerging applications, including superconductors, thermoelectrics, fuel cells, batteries, and solar cells, fabricated through a variety of techniques including ultra-high-pressure synthesis and atomic and molecular layer deposition. Karppinen was nominated as Academy Professor in Finland for 2009–2013, and in 2013 she received her ERC Advanced Grant for ALD/MLD inorganic-organic materials, followed by ERC proof-of-concept grants for flexible thermoelectrics and Li-organic microbattery.